

Optimizing 3D printing parameters to improve dimensional accuracy

Sabi Sabev

Technical University of Sofia,
Branch Plovdiv
Plovdiv, Bulgaria
sabi_sabev@tu-plovdiv.bg

Konstantin Chukalov

Technical University of Sofia,
Branch Plovdiv
Plovdiv, Bulgaria
chukalov@tu-plovdiv.bg

Valeri Bakardzhiev

Technical University of Sofia,
Branch Plovdiv
Plovdiv, Bulgaria
bakardzhiev@tu-plovdiv.bg

Agop Izmirliyan

Technical University of Sofia,
Branch Plovdiv
Plovdiv, Bulgaria
izmirliyan@tu-plovdiv.bg

Abstract. The article examines the influence of 3D printing speed and layer thickness on the accuracy of functional dimensions of a part-eight wall prism with 5 holes-one in the centre and 4 in the periphery. For printing the samples, ABS material was used, which is one of the main materials for the production of machines and parts. A portal measuring machine with the highest accuracy was used to effectively perform the task of measuring deviations from the size of the sample. Due to the large volume of experimental results, they were averaged to minimize error and processed using statistical processing software. An accurate regression model was obtained and the printing parameters were optimized

Keywords: 3D printing, dimension accuracy

I. INTRODUCTION

3D printing is increasingly used in many sectors - mechanical engineering, architecture, design, dentistry [1],[2]. 3D printing is used not only for prototyping, but also for mass production [3]. The materials that are used for this technology are very diverse, but mostly polymers are Acrylonitrile Butadiene Styrene (ABS), Polystyrene (HIPS) and Polylactic Acid (PLA) [4],[5]

The main technological characteristics of the process are the height of the layer and the printing speed, on which the quality of the 3d printed details mainly depends. 3D printing is a developing scientific field[6]

Geometric deviations are defined as a deviation from the ideal geometry of the part. Size deviation is a deviation from the local size (the distance between two

points on the surface)[7]. Different systems are used to ensure accuracy[8].

The increasingly wide application of 3D printing leads to increased requirements for the characteristics of the details, as well as the analysis of technological operations.[9].

II. MATERIALS AND METHODS

The material used is the polymer Acrylonitrile butadiene styrene (ABS) chemical formula $(C_8H_8)_x \cdot (C_4H_6)_y \cdot (C_3H_3N)$ [10]. The choice of material is determined by the wide use of this material in 3D printing. [11]. The material is pre-extruded into a layer (filament with a diameter of 1.75 mm). In the printing process, the polymer is extruded at a temperature of 235°C. The selected part is eight wall prism with 5 holes. This shape is selected to satisfy the goals of the article. The 3D printer and the process in the Flashforge Creator model are shown in Figure 1.

The planning of the experiment has been done in previous articles and is according to the Taguchi method: Taguchi Array L9 (3^2); Factors: 2; Runs: 9

The limits (maximum and minimum value) of the factors affecting the quality and accuracy of printing are determined a priori.[12] Factors investigated for impact on accuracy are print speed and layer height[13] The 3D printer parameters that are constant for all trials, ie. are constant: nozzle diameter 0.4mm; flow 100%; retreat 1mm; bed temperature 110°C.

Print ISSN 1691-5402

Online ISSN 2256-070X

<https://doi.org/10.17770/etr2024vol3.8146>

© 2024 Sabi Sabev, Konstantin Chukalov, Valeri Bakardzhiev, Agop Izmirliyan.

Published by Rezekne Academy of Technologies.

This is an open access article under the [Creative Commons Attribution 4.0 International License](https://creativecommons.org/licenses/by/4.0/).

- Checking dimension deviations according the 3D model



Fig. 1. Flashforge Creator 3

The measurement was carried out on a three-coordinate measuring machine EROWA CMM QI, which is designed for the control of finished parts. The machine is placed in a temperature controlled environment of 20°C ±1°. It is equipped with a contact sensor TP20 and a ruby sphere D=6mm. (fig. 2). The technical parameters are:

$$r = 0.0001 \quad (1)$$

$$T = 1.5\mu\text{m} + L/500 \quad (2)$$

(where: r – resolutions; T-tolerance field of the measurement; L-length of the measured dimension in mm)



Fig. 2. TP20 sensor with D6 probe.

- Software

The software used to check deviations from the 3D model is ARCO CAD. The IGS format is used to extract the geometric data of the specimen. A control program was developed to touch each sample at the same point relative to the set base, with the same speed of movement of the sensor. This prevents the possibility of accumulating additional measurement errors. (fig.3)

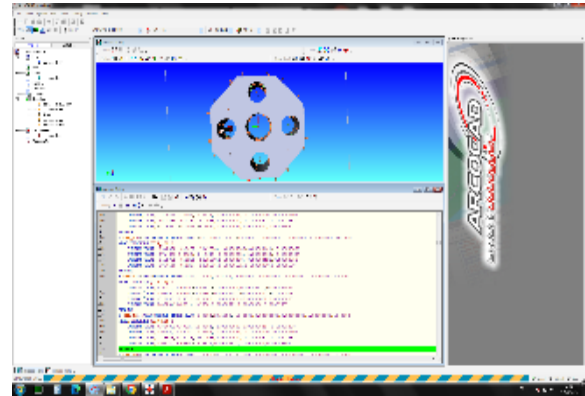


Fig. 3. Arco CAD software overview

- Fastening

The specimen is fixed on the outer two walls and its front surface in a precision self-centering vise (fig4). The central opening O0 a for the Z coordinate – the front surface P – is chosen as a base for the X and Y coordinates.

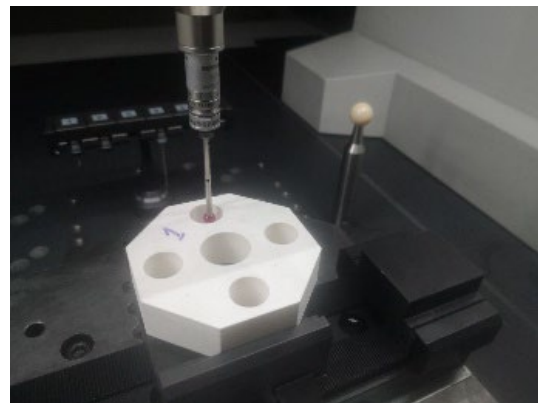


Fig. 4. Fixture set up on measuring machine.

For the purpose of the experiment, 4 measurements were made on each hole of each specimen[14] The circumference measurement was done with a 4 contact point circumference measuring cycle. The first 2 measurements are at a depth of Z=-5mm and the second 2 at Z=-15mm. The difference between measurement 1 and 2, as well as 3 and 4 is the starting angle of measurement ($\alpha=45^\circ$). Fig(5.a) In this way, we have also extracted information about the average deviation from the shape of the corresponding hole. In addition to diameter and shape deviation, we have also measured the average deviation of the interaxial distance of each hole relative to the central hole, which serves as the base and origin of our coordinate system. (table 1)

- Checking of external faces

The external shape of the experimental sample is octahedral composed of 8 planes respectively. In fact, the planes from which the geometric body is created after printing deviate in shape and location from those in the specified computer model [15],[16]. Through an option to match a given point from the imported 3D model in the Arco cad software and the actually touched point from the sensor, the average deviation of 4 points for each wall of the octagon was measured, each of them being at the maximum distance from each other. (Fig.5 .b)

In this way, the error of the positioning of the wall itself relative to the mathematical model and also the differences in the shape of the real surface of the specimen are combined[17]. The results of the measured points are averaged for each wall of the octagon of each specimen. (Table 2)

- Measurement of the front surface

3 points from the front surface of each specimen were measured. The base surface is the face of the first sample (fig. 5.c) (Table 3)

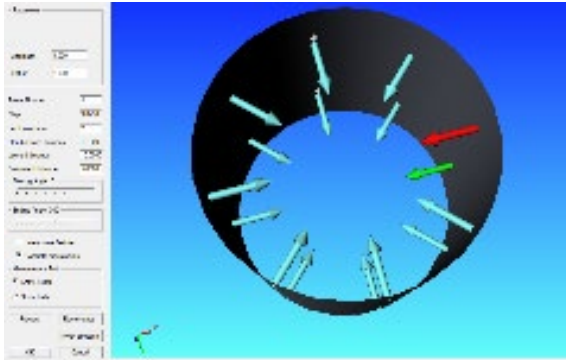


Fig. 5. (a) 16 measuring points for each cylinder

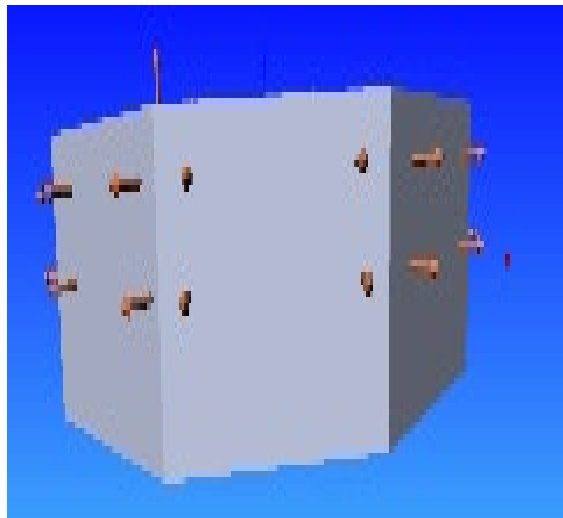


Fig.5 (b) 4 points on each side of the octagon

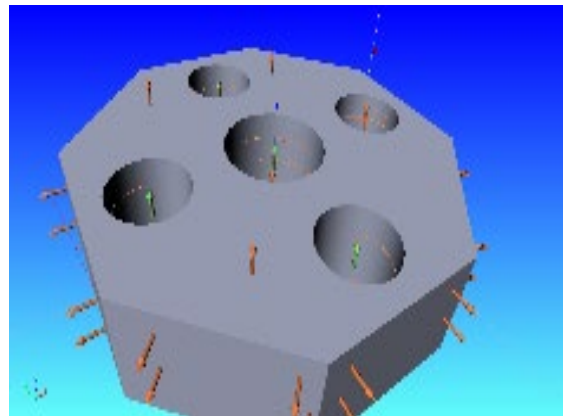


Fig.5 (c) 3 points taken from the face surface

III. RESULTS AND DISCUSSION

Table 1. Diameters of the measured holes and the coordinates of their interaxial distances.

TABLE 1 DIAMETERS OF THE MEASURED HOLES AND THE COORDINATES OF THEIR INTERAXIAL DISTANCES.

		Sample 1	Sample 2	Sample 3	Sample 4	Sample 5	Sample 6	Sample 7	Sample 8	Sample 9
D1	D	21,82	21,75	21,64	21,64	21,61	21,57	21,67	21,67	21,65
	D	15,83	15,76	15,65	15,65	15,66	15,55	15,76	15,74	15,67
D2	X	27,07	27,22	27,34	27,30	27,29	27,36	27,22	27,35	27,28
	Y	-0,03	0,07	-0,04	-0,03	0,04	-0,07	0,08	-0,09	-0,14
D3	D	15,89	15,82	15,68	15,69	15,59	15,53	15,72	15,70	15,67
	X	-27,18	-27,28	27,26	-27,31	-27,27	-27,24	-27,16	-27,09	27,22
D4	Y	-0,08	-0,08	-0,07	0,05	-0,09	-0,07	-0,07	-0,23	-0,11
	D	15,87	15,78	15,71	15,71	15,61	15,52	15,87	15,71	15,64
D5	X	-0,03	-0,05	0,05	-0,01	0,01	0,04	-0,02	0,12	0,03
	Y	27,50	27,46	27,43	27,41	27,39	27,28	27,53	27,33	27,32
D5	D	15,87	15,80	15,68	15,68	15,61	15,57	15,73	15,73	15,71
	X	-0,06	-0,01	0,02	0,01	0,02	0,07	0,03	0,15	0,03
D5	Y	-27,61	-27,48	-27,34	-27,37	-27,45	-27,45	-27,49	-27,62	-27,55

TABLE 2. AVERAGE DEVIATION OF WALLS FROM 3D MODEL

Sample	SIDE							
	1	2	3	4	5	6	7	8
1	-0,33	-0,08	-0,08	-0,17	-0,38	-0,15	-0,05	-0,17
2	-0,34	-0,17	-0,04	-0,16	-0,24	-0,09	-0,06	-0,20
3	-0,19	-0,23	-0,15	-0,03	-0,08	-0,10	-0,12	-0,14
4	-0,14	-0,14	-0,08	-0,03	-0,10	-0,18	-0,18	-0,14
5	-0,17	0,11	0,19	-0,01	-0,26	-0,31	-0,31	-0,32
6	-0,16	-0,16	-0,20	-0,14	-0,16	-0,16	-0,08	-0,08
7	-0,30	-0,07	-0,01	-0,21	-0,37	-0,14	0,02	-0,14
8	-0,32	-0,06	0,07	-0,09	-0,28	-0,21	-0,17	-0,30
9	-0,19	-0,21	-0,21	-0,24	-0,28	-0,17	-0,01	-0,02

TABLE 3. AVERAGE DEVIATION OF FOREHEAD FROM 3D MODEL

Sample	1	2	3	4	5	6	7	8	9
Result	0,04	-0,10	-0,37	-0,21	-0,29	-0,28	-0,27	-0,23	-0,39

TABLE 4 EXPERIMENTAL RESULTS FOR DEVIATION OF THE SIZE

№	Layer	Speed	Def dD
1	0,1	10	0,14
2	0,1	45	0,22
3	0,1	80	0,43
4	0,25	10	0,33
5	0,25	45	0,38
6	0,25	80	0,45
7	0,4	10	0,28
8	0,4	45	0,29
9	0,4	80	0,33

The obtained experimental results for the size deviation are presented in Table. 1-4. Table 4 presents the arithmetic mean deviation of the size.

Mathematical-statistical processing was performed with MINITAB 19 software. For the mathematical description of the objective function, a reduced model of the second incomplete degree was used.

The data from Table 4 were processed and the following regression model was obtained [15]:

$$Def\ dD = -0.034 + 2.457\ layer + 0.002231\ Speed - 4.68\ layer * layer \quad (3)$$

The coefficient of determination R-sq = 77.10% was calculated, and the adjusted coefficient of determination has the value R-sq(adj) = 63.36%, which is too low.

TABLE 5 MODEL SUMMARY

S	R-sq	R-sq(adj)	PRESS	R-sq(pred)	AICc	BIC
0.060	77.10%	63.36%	0.068	13.47%	-0.39	19.41

TABLE 6 ANALYSIS OF VARIANCE

Source	DF	Seq SS	Contribution	Adj SS	Seq MS	F-Value	P-Value
Regression	3	0.061	77.10%	0.061	0.020	5.61	0.047
layer	1	0.001	2.27%	0.023	0.001	0.50	0.513
Speed	1	0.036	46.55%	0.036	0.036	10.16	0.024
layer*layer	1	0.022	28.28%	0.022	0.022	6.17	0.056
Error	5	0.017	22.90%	0.017	0.003		
Total	8	0.078	100.00%				

The Pareto chart, Fig.6 shows the absolute values of the standardized effects from largest to smallest effect.[16] The chart also draws a reference line to show which effects are statistically significant.[17] It can be seen that component B has crossed the significance line, therefore only this coefficient is insignificant and the rest are insignificant.

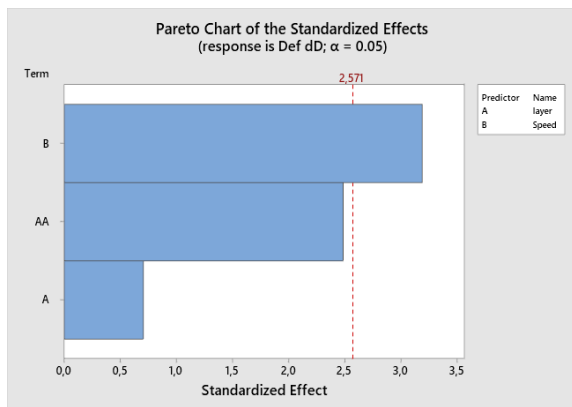


Fig. 6. Pareto Chart

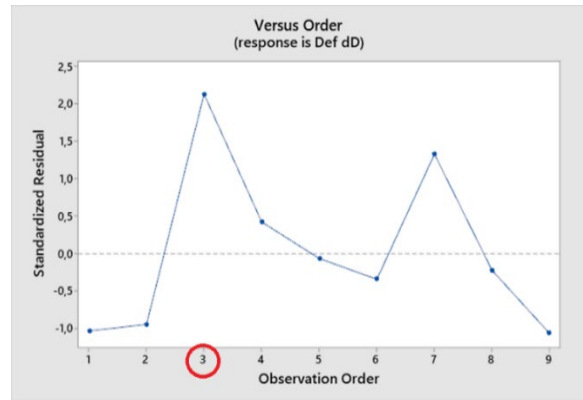


Fig. 7. Versus order residual

Fig. 7 clearly shows the presence of 1 error: - observation No. 3, the value of the standardized residual should be within the limits of -2;+2. This gives us reason to remove the observation and process the data again.

After reprocessing the results we get the following Regression Equation:

$$Def\ dD = -0.1290 + 3.324\ layer + 0.001374\ Speed - 6.017\ layer * layer \quad (4)$$

The coefficient of determination R-sq = 97.16% was calculated, and the adjusted coefficient of determination has the value R-sq(adj) = 95.03%, which satisfies the requirement of being above 95%. The P-value must be below 0.05, this condition is also met.

Suppose we want to know if this F statistic is significant at level alpha = 0.05. Using the F-distribution table for alpha = 0.05, with numerator of degrees of freedom 3 (Regression) and denominator degrees of freedom 4 (Error), we find that the F critical value is 6.5914. [18]. From the analysis of the variables in table 10, it can be seen that all the F-values are several times above the critical value.

TABLE 7 MODEL SUMMARY

S	R-sq	R-sq(adj)	PRESS	R-sq(pred)	AICc	BIC
0.021	97.16%	95.03%	0.009	86.20%	-4.47	-34.08

TABLE 8 ANALYSIS OF VARIANCE

Source	DF	Seq SS	Contribution	Adj SS	Seq MS	F-Value	P-Value
Regression	3	0.061	97.16%	0.062	0.021	45.6	0.001
layer	1	0.011	17.62%	0.037	0.011	24.8	0.008
Speed	1	0.017	27.60%	0.010	0.017	38.8	0.003
layer*layer	1	0.033	51.95%	0.033	0.033	73.1	0.001
Error	4	0.002	2.84%	0.002	0.001		
Total	7	0.063	100.00%				

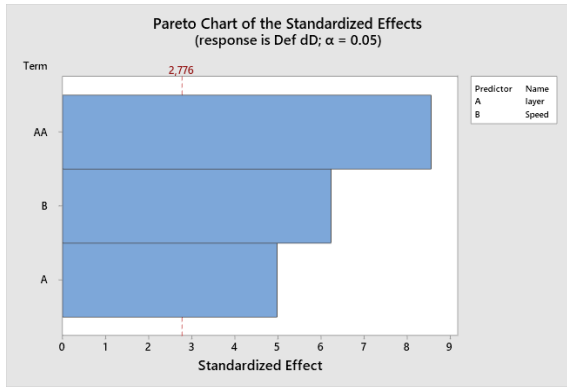


Fig. 8. Pareto Chart

The Pareto diagram, Fig. 8 shows that the components have crossed the significance line, therefore all the coefficients are significant.

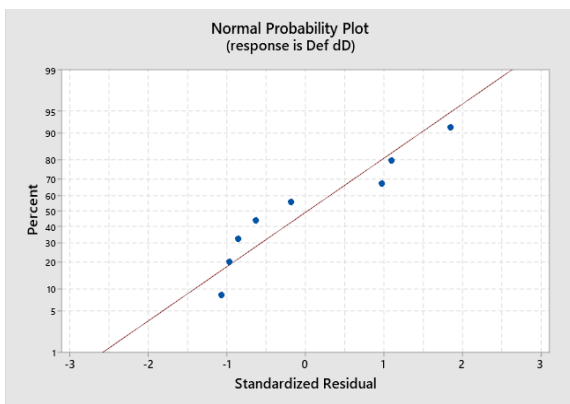


Fig. 9. Normal probability plot

The analysis of standardized residuals Fig. 9 - 10, shows that there are no gross errors. This necessitates the conclusion that the coefficients are significant.

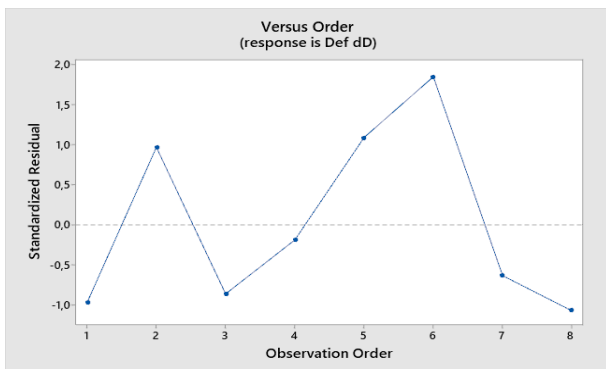


Fig. 10. Versus Order

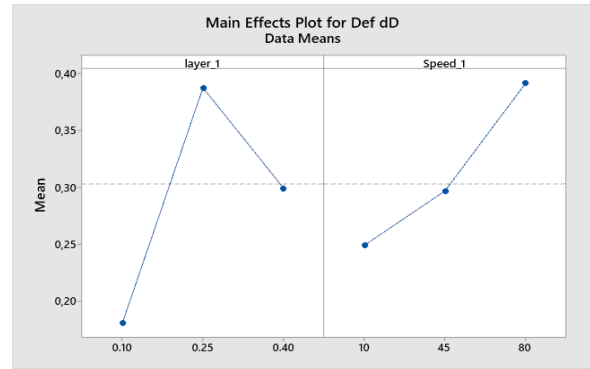


Fig. 11. Main effect

It was also analyzed how the influence of layer and speed on the size deviation, fig. 11-12

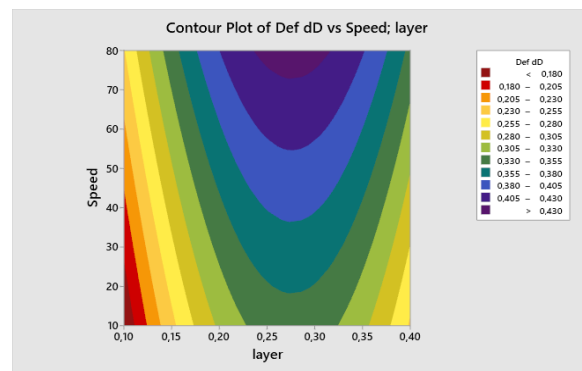


Fig. 12. Contur plot

The interactive table, Fig.13 shows the effect of layer and print speed on the printing time.

A one-parameter optimization was made, with the optimization criteria being the printing time of 4 hours and the size deviation being equal to 0.25mm. The obtained results are presented in Fig. 14 with a deviation of 0.25 mm, i.e. tolerance field $\pm 0.125\text{mm}$, layer thickness 0.35mm, the time for printing the part is 4 hours. The following regression model was used in this optimization:

$$\text{Time}[h] = 11.26 - 12.39\text{Def}dD[\text{mm}] - 11.91 \text{ layer} \quad (5)$$

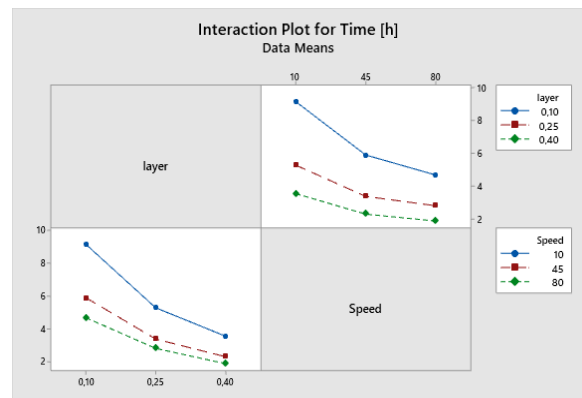


Fig. 13. Interactive plot

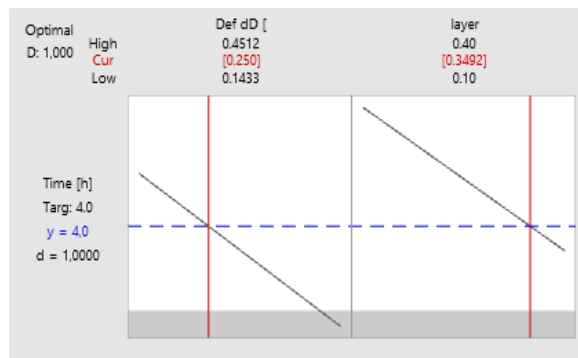


Fig. 14. Optimization plot

IV. CONCLUSIONS

The research is executed on base of statistical process according Taguchi method - 9 samples are manufactured for this goal. The printing modes are selected according to the importance of technology. The following conclusions are drawn from the statistical processing:

1. The greatest influence of layer height is observed on dimension deviation
2. The printing speed has a minor influence on the dimension deviation
3. The study can be used as a basis for another discrete area of the studied parameters.
4. All regression models are notable and well describe the relationship between printing speed and layer height.

The studied polymer material ABS, one of the current polymers, is used for the production of technical details.

V. ACKNOWLEDGMENTS

The author/s would like to thank the Research and Development Sector at the Technical University of Sofia for the financial support.

VI. REFERENCES

[1] S. Choi, Y. Bae, I. Lee, H. Kim, Latest Research Trends of 3D Printing in Korea, Journal of the Korean Society for Precision Engineering - Vol. 35, No. 9, pp. 829-834, 2018 <https://doi.org/10.7736/KSPE.2018.35.9.829>

[2] M. Jeoung, M. Ramodski, D. Lopez, J. Liu, J. Lee, S. Lee, Materials and Applications of 3D Printing Technology in Dentistry: An Overview, Dentistry Journal 12(1):1, Dentistry Journal 12(1):1, 2023 <https://doi.org/10.3390/dj12010001>

[3] S. Ragan, Plastics for 3D Printing, MAKE, 2013

[4] Ultimate Guide To 3D Printing, Winter, pp. 22; <http://makezine.com/2012/11/13/plastics-for-3d-printing/.2013>

[5] M. Subramaniyan, S. Karuppan, Mechanical properties of sandwich products obtained by 3D printing from PLA-PLA/Al₂O₃, Polimery 68 (11-12):646-651,, <https://doi.org/10.14314/polimery.2023.11.9>, 2023

[6] D. Rathia, International Journal of Innovative Science and Research Technology Volume 8 - 2023, (Issue 7 - July) <https://doi.org/10.5281/zenodo.8216770>, 2023

[7] S. Eom, J. Park, J. Jin, J. Son, Feasibility Study on Dimensional Standard for Material Extrusion Type 3D Printed Structures, Journal of the Korean Society for Precision Engineering - Vol. 37, No. 4, pp. 241-246, 2020 <https://doi.org/10.7736/JKSPE.019.118>

[8] V. Georgiev, S. Salapateva, I. Chetkov, S. Lilov, Systems for ensuring the accuracy of the dimensions of details in mechanical engineering on CNC machines. International Conference "Automation and Informatics'08", Collection of reports, Sofia, 2008, pp. V-15 - V-18, 2008

[9] A. Mahmood, T. Akram, H. Chen, S. Chen, On the Evolution of Additive Manufacturing (3D/4D Printing) Technologies: Materials, Applications, and Challenges, Polymers 14(21):4698, 2020 <https://doi.org/10.3390/polym14214698>

[10] E. N. Peters, "Plastics: Thermoplastics, Thermosets, and Elastomers", Handbook of Materials Selection, New York: John Wiley & Sons, Inc., pp. 363-365, 2007

[11] F. Ballarin, A. Lola, A. Irawan, N. Kikuchi, B. Chouangthavy Find your way out of the ABS maze: three cases of successful Access and Benefit Sharing compliance, 2023

[12] Y. Mayorava, V. Sikulskiy, I. V. Vorobiov, A. Knys, Study of a Geometry Accuracy of the Bracket-Type Parts Using Reverse Engineering and Additive Manufacturing Technologies, 2023 <https://doi.org/10.3390/app132212200>

[13] P. Barve, A. Bahrami, S. Shah, Geopolymer 3D printing: a comprehensive review on rheological and structural performance assessment, printing process parameters, and microstructure, Frontiers in Materials 10:1241869, 2023 <https://doi.org/10.3389/fmats.2023.1241869>

[14] D. Popescu, C. Amza, R. Marinescu, M. Iacob, N. Carotasu, Investigations on Factors Affecting 3D-Printed Holes Dimensional Accuracy and Repeatability, Applied Sciences 13(1):41, 2023 <https://doi.org/10.3390/app13010041>

[15] S. Satin, G. Goodacre, R. Masri, Comparing the accuracy of occlusal vertical dimension transfer in CAD-CAM dentures Journal of Prosthodontics, 2023 <https://doi.org/10.1111/jopr.13669>

[16] A. Wang, C. Ruiz, S. Park, K. Shin, J. Kim, Q. Huang ASME 2022 17th International Manufacturing Science and Engineering Conference, 2023 <https://doi.org/10.1115/MSEC2022-FM1>

[17] T. Morita, S. Watanabe, S. Sasake, Multi-axis printing method for bent tubular structured gels in support bath for achieving high dimension and shape accuracy, Precision Engineering 79, 2022 <https://doi.org/10.1016/j.precisioneng.2022.09.004>

[18] H. Ishikawa, Regression, Hypothesis Generation and Interpretation, 2024 https://doi.org/10.1007/978-3-031-43540-9_4